Published in final edited form as:
Inorg Chem. 2011 May 16; 50(10): 4256–4259. doi:10.1021/ic101772d.

Electronic Properties and ^{13}C NMR Structural Study of $Y_3N@C_{88}$

Wujun Fu, **Jianyuan Zhang**, **Hunter Champion**, **Tim Fuhrer**, **Hugo Azuremendi**, **Tianming Zuo**, **Jianfei Zhang**, **Kim Harich**, and **Harry C. Dorn***
Department of Chemistry, Virginia Polytechnic Institute and State University, Blacksburg, VA, 24061, USA

Abstract

In this paper we report the synthesis, purification, ^{13}C NMR and other characterization studies of $Y_3N@C_{88}$. The ^{13}C NMR, UV-vis and chromatographic data suggest an $Y_3N@C_{88}$ having IPR allowed cage with $D_2(35)$-C_{88} symmetry. In earlier density functional theory (DFT) computational and X-ray crystallographic studies, it was reported that lanthanide $(A_3N)^{6+}$ clusters are stabilized in $D_2(35)$-C_{88} symmetry cages and have reduced HOMO-LUMO gaps relative to other trimetallic nitride endohedral metallofullerene cage systems, for example, $A_3N@C_{80}$. In this paper, we report that the non-lanthanide $(Y_3N)^{6+}$ cluster in the $D_2(35)$-C_{88} cage exhibits a HOMO-LUMO gap consistent with other lanthanide $A_3N@C_{88}$ molecules based on electrochemical measurements and DFT computational study. These results suggests that the reduced HOMO-LUMO gap of $A_3N@C_{88}$ systems is a property dominated by the $D_2(35)$-C_{88} carbon cage and not f-orbital lanthanide electronic metal cluster $(A_3N)^{6+}$ orbital participation.

Introduction

The separation and characterization of higher fullerenes beyond C_{80} is very difficult, not only because of their extremely low yield, but also the possible presence of multiple isomers, instability, and lower solubility.[1] For example, Yang *et al.* reported the separation of Di-and Tridysprosium Endohedral Metallofullerenes in the fullerene cages from C_{94} to C_{100}.[2] Due to the limited available amount of sample, they did not obtain any structural information of those large cages. [2] Among the large fullerene cages, the C_{88} cage has been widely studied. As early as 1995, C_{88} empty cage fullerenes were separated from soot generated in a Kratschmer-Huffman electric-arc generator and subsequently characterized using ^{13}C NMR by Achiba *et al.*[3] In a later report, Miyake *et al.*[4] described a more detailed ^{13}C NMR study for the C_{88} empty cage fullerene. However, the structural assignments were ambiguous because at least three C_{88} isomers exist.[4] Due to the difficulty in experimental part, the extensive theoretical studies were performed by several groups to aid the structural determination.[5,6] It was predicted that $C_2(7)$, $C_s(17)$ and $C_2(33)$ isomers are the mostly likely to be experimentally-isolated isomers among the 35 IPR-obeying isomers of C_{88}.[5,6] Derivatization of empty fullerene cages has proved to be an effective tool for cage stabilization and meanwhile provides a path for further structural characterization. For example, Troyanov and Tamm [7] synthesized and characterized trifluoromethyl derivatives of C_{88}, $C_{88}(CF_3)_{18}$. Based on their X-ray investigation, they determined that $C_{88}(CF_3)_{18}$ processes a $C_2(33)$-C_{88} cage, which is one of the three most stable isomers predicted on a theoretical basis. Encapsulation of atoms or clusters into fullerene cages is another method used to stabilize empty fullerene cages by electron transfer processes between the encapsulated and the carbon cage.

*Author to whom correspondence should be addressed; hdorn@vt.edu, Fax: 540-231-3255, Tel: 540-231-5953.

Trimetallic nitride template (TNT) endohedral metallofullerenes (EMFs) are particularly important not only because of their relatively high yields, but also because of their intriguing potential applications in biomedical, optoelectronic, and photovoltaic fields.[8,9] Insertion of a TNT cluster into a C_{88} cage ($M_3N@C_{88}$, M= Gd, Tm, Dy, Tb, Nd, Pr, Ce, La) has been reported by several laboratories.[10–13] Echegoyen and coworkers suggested that the C_{88} cage is preferentially templated by a TNT cluster for metal ions with ionic radius larger than gadolinium, such as, Nd, Pr, Ce.[10,11] However, most of the TNT EMFs with the C_{88} cage have been characterized by mass spectroscopy without definitive structural characterization. Notable exceptions are the single crystal X-ray studies reported for $Tb_3N@C_{88}$ which have been found to have an IPR-obeying $D_2(35)$ structure.[12] This is in contrast with the theoretical predictions for the empty C_{88} cage. Thus, it is interesting to examine whether clusters with different metals $(A_3N)^{6+}$ encapsulated within a C_{88} cage have the same cage structure as IPR-obeying $Tb_3N@D_2(35)$-C_{88}.

In this paper, we report the synthesis, separation and structural characterization of diamagnetic $Y_3N@C_{88}$. This diamagnetic molecule allows high-resolution ^{13}C NMR structural studies, which are generally not feasible for the paramagnetic lanthanide C_{88} cage TNT EMFs reported above. Density function theory calculations were utilized to augment the structural determination. The electronic properties of $Y_3N@C_{88}$ were also studied by both electrochemical and DFT computational approaches to compare a non-lanthanide TNT EMF with the corresponding lanthanide TNT EMFs reported to date.

Experimental Section

A sample of $Y_3N@C_{88}$ was synthesized in an electric arc-discharge reactor by vaporizing graphite rods containing a mixture of Y_2O_3 and graphite powder and using Cu as catalyst with a weight ratio of 1.1:1.0:2.1 in a dynamic flow of N_2 and He (flow rate ratio of N_2/He=3:100).[14] The toluene extract from the raw soot was applied to a cyclopentadiene-functionalized Merrifield peptide resin. The eluent was further separated by two-stage HPLC. The first stage was carried out on a 5PBB column and the sixth fraction contains $Y_3N@C_{88}$, which was further purified by a 5PYE column.

The ^{13}C NMR measurements (150 MHz) were performed on a Bruker Advance spectrometer (600 MHz, ^1H). The sample was dissolved in CS_2 with $Cr(acac)_3$ as the relaxation agent and acetone-d_6 as the internal lock at 25 °C. Cyclic voltammetry was conducted using a CH Instruments 600A potentiostat (Austin, TX) with a single-compartment, three electrode, electrochemical cell. A 2.0 mm glassy carbon working electrode, platinum wire auxiliary, and a silver wire pseudo-reference electrode was used; ferrocene was used as an internal standard.

Density functional theory (DFT) computations were performed using the Gaussian 03 program package. All of the molecules were geometrically optimized at the UB3LYP level with a DZVP basis set for yttrium atoms and a 6-31G* basis set for carbon and nitrogen atoms.[14] DFT-optimized energy values were obtained starting from the X-ray crystallographic structures of the corresponding $Tb_3N@D_2(35)$-C_{88}.[11]

Results and Discussion

As illustrated in Figure 1, the HPLC, positive ion LD-TOF MS, and UV-vis spectra for $Y_3N@C_{88}$ is compared with data that was previously reported for $Tb_3N@C_{88}$.[12] The close correspondence of the data in Figure 1 strongly suggests that $Y_3N@C_{88}$ has the same $D_2(35)$cage structure as $Tb_3N@D_2(35)$-C_{88}.[12] Because the $Y_3N@C_{88}$ molecule is diamagnetic, we were able to obtain high-resolution ^{13}C NMR data for $Y_3N@C_{88}$ to further confirm the cage structure.

The ^{13}C NMR spectrum (Figure 2a) for $Y_3N@C_{88}$ exhibits a total of 22 lines (lines at 139.10 and 139.69 ppm, double intensity) with a shift range from 131.0 to 150.0 ppm. This result is completely consistent with the 22 ^{13}C NMR signals observed for $Y_3N@C_{88}$. An IPR-allowed isomer is suggested because of the absence of a ^{13}C NMR signal above 155 ppm, which is characteristic of non-IPR pentalene motifs.[14] There are 35 IPR-allowed C_{88} isomers and two isomers (1) and (35) that have D_2 symmetry (22 × 4 lines) which is consistent with the observed spectrum.[15] Among the 35 IPR-obeying isomers for the C_{88} cage, no other IPR-allowed structure would exhibit fewer than 22 lines except for isomer (34) with T symmetry that would exhibit 8 ^{13}C NMR resonances (1×4 and 7×12). All other C_{88} IPR isomers have lower symmetry and would exhibit more than 22 spectral lines. In addition, there are 7 pyrene 6,6,6 type carbons that range from 132.0–137.9 ppm, which is in reasonably good agreement with 7 DFT predicted values (Figure 2b) ranging from 131.9–139.2 ppm.[14] The correlation between experimental ^{13}C and the DFT predicted chemical shielding values are shown in Figure 2c. $Tb_3N@D_2(35)$-C_{88} exhibits a carbon cage with D_2 symmetry as determined by previous single-crystal X-ray diffraction studies. Thus, our current results are consistent with a $Y_3N@D_2(35)$-C_{88} structure in analogous fashion to $Tb_3N@D_2(35)$-C_{88}.[12]

As previously indicated, there are three isomers of empty-cage C_{88} cage, $C_2(7)$, $C_s(17)$ and $C_2(33)$, that are predicted to be thermodynamically and kinetically stable.[5,6] However, C_{88} with $D_2(35)$ symmetry is not included in this group. Computational calculations (DFT) summarized in Figure 3 suggest that the neutral IPR $D_2(35)$-C_{88} has a small HOMO-LUMO gap (1.27 eV), indicating the lower stability of the neutral $D_2(35)$-C_{88} cage. However, upon accepting six electrons, the HOMO-LUMO gap becomes significantly larger (1.77 eV), consistent for higher stability of the $Y_3N@D_3(35)$-C_{88} molecule. To our knowledge, neither the Y_3N cluster or the $D_2(35)$-C_{88} cage have been isolated, but when associated together, they form a stable $Y_3N@D_3(35)$-C_{88} structure by electron transfer between the cluster and the cage.

As illustrated in Figure 4, the CV electrochemistry of $Y_3N@C_{88}$ and $Gd_3N@C_{88}$ are nearly equivalent. The $Gd_3N@C_{88}$ sample for this CV electrochemistry comparison was isolated and purified (see SI) in the same fashion as described for $Y_3N@C_{88}$ *vide supra* and is consistent with previously reported data by Echegoyen and coworkers.[16] The electrochemistry of $Y_3N@C_{88}$ and $Gd_3N@C_{88}$ can be described as having two distinct oxidative processes accompanied by a first and second reduction peak potential of −1.43 V and −1.70V, respectively. Redox potentials and resulting electrochemical gap (ΔE_{gap}) for $Y_3N@C_{88}$ are in good agreement with reported literature values for other $M_3N@C_{88}$ systems (Table 1). This is consistent with a single (non-degenerate) LUMO level for $Y_3N@C_{88}$ obtained from the DFT calculations described above. The resulting electrochemical bandgap ($^{ox}E_1$-$^{red}E_1$) for the $Y_3N@C_{88}$ is 1.46 V, reasonably consistent with the DFT predictions above. Although ($^{ox}E_1$-$^{red}E_1$) for $Y_3N@C_{88}$ is smaller than the more stable $Y_3N@C_{80}$ case,[16] this bandgap is similar to other $M_3N@C_{88}$ family members, such as, $Gd_3N@C_{88}$ (1.49 V),[17] $Nd_3N@C_{88}$ (1.43 V),[11] $Pr_3N@C_{88}$ (1.43 V),[9] $Ce_3N@C_{88}$(1.38 V)[9] and $La_3N@C_{88}$(1.57 V)[9]. These results suggests that the ($^{ox}E_1$-$^{red}E_1$) bandgap (and corresponding HOMO-LUMO gap) of $A_3N@C_{88}$ trimetallic nitride endohedral metallofullerenes is a property dominated by the properties of the $D_2(35)$-C_{88} carbon cage and not the nature of the yttrium or lanthanide electronic metal cluster $(A_3N)^{6+}$.

Conclusion

In summary, we have synthesized, purified and characterized diamagnetic $Y_3N@C_{88}$ for the first time. The ^{13}C NMR study indicates that $Y_3N@C_{88}$ exhibits an IPR-obeying $D_2(35)$-C_{88} cage. The electrochemical data suggested that $Y_3N@C_{88}$ has a smaller HOMO-LUMO

gap than $Y_3N@C_{80}$ which is consistent with the computational DFT study. Also, our results show that encapsulation of an Y_3N cluster does not significantly alter the electrochemical properties of these trimetallic nitride endohedral metallofullerenes and this result is consistent with other lanthanide M_3N clusters in $D_2(35)$-C_{88} cages. This suggests that the unique $D_2(35)$-C_{88} cage properties strongly influence the electrochemical and electronic properties of these trimetallic nitride endohedral metallofullerenes.

Supplementary Material

Refer to Web version on PubMed Central for supplementary material.

Acknowledgments

We gratefully acknowledge support by the National Science Foundation [CHE-0443850 (H.C.D.), DMR-0507083 (H.C.D.)] and the National Institutes of Health [1R01-CA119371-01 (H.C.D.)]. We would also like to acknowledge Dr. Jiechao Ge for his help with some of the preparation for this work.

References

1. Popov AA, Dunsch L. J Am Chem Soc. 2007; 129:11835–11849. [PubMed: 17760444]
2. Yang S, Dunsch L. Angew Chem Int Ed. 2006; 45:1299–1302.
3. Achiba, Y.; Kikuchi, K.; Aihara, Y.; Wakabayashi Miyake, Y.; Kainosho, M. Science and Technology of Fullerene Matrials. In: Bernier, P.; Bethune, DS.; Chiang, LY.; Ebbesen, TW.; Metzger, RM.; Mintmire, JW., editors. MRS Symposia Proceedings No. 359. 1995. p. 3-9.
4. Miyake Y, Minami T, Kikuchi K, Kainosho M, Achiba Y. Mol Cryst Liq Cryst. 2000; 340:553–558.
5. Watanabe M, Ishimaru D, Mizorogi N, Kiuchi M, Aihara JI. Theochem. 2005; 726:11–16.
6. Sun GY. Chem Phys Lett. 2003; 367:26–33.
7. Troyanova S, Tamm NB. Chem Comm. 2009:6035–6037. [PubMed: 19809635]
8. Fatouros PP, Corwin FD, Chen ZJ, Broaddus WC, Tatum JL, Kettenmann B, Ge ZX, Gibson HW, Russ JL, Leonard AP, Duchamp JC, Dorn HC. Radiology. 2006; 240:756–764. [PubMed: 16837672]
9. Ross RB, Cardona CM, Guldi DM, Sankaranarayanan SG, Reese MO, Kopidakis N, Peet J, Walker B, Bazan GC, Van Keuren E, Holloway BC, Drees M. Nature Mater. 2009; 8:208–212. [PubMed: 19202546]
10. Chaur MN, Melin F, Elliott B, Kumbhar A, Athans AJ, Echegoyen L. Chem Eur J. 2008; 14:4594–4599.
11. Melin F, Chaur MN, Engmann S, Elliott B, Kumbhar A, Athans AJ, Echegoyen L. Angew Chem Int Ed. 2007; 46:9032–9035.
12. Zuo TM, Beavers CM, Duchamp JC, Campbell A, Dorn HC, Olmstead MM, Balch AL. J Am Chem Soc. 2007; 129:2035–2043. [PubMed: 17256857]
13. Yang SF, Dunsch L. J Phys Chem B. 2005; 109:12320–12328. [PubMed: 16852521]
14. Fu WJ, Xu LS, Azurmendi H, Ge JC, Fuhrer T, Zuo TM, Reid J, Shu CY, Harich K, Dorn HC. J Am Chem Soc. 2009; 131:11762–11769. [PubMed: 19639998]
15. Fowler, PW.; Manolopoulos, DE. An Atlas of Fullerenes. Clarendon Press; Oxford: 1995.
16. Cardona CM, Elliott B, Echegoyen L. J Am Chem Soc. 2006; 128:6480–6485. [PubMed: 16683813]
17. Charu MN, Melin F, Elliott B, Athans AJ, Walker K, Holloway BC, Echegoyen L. J Am Chem Soc. 2007; 129:14826–14829. [PubMed: 17983231]

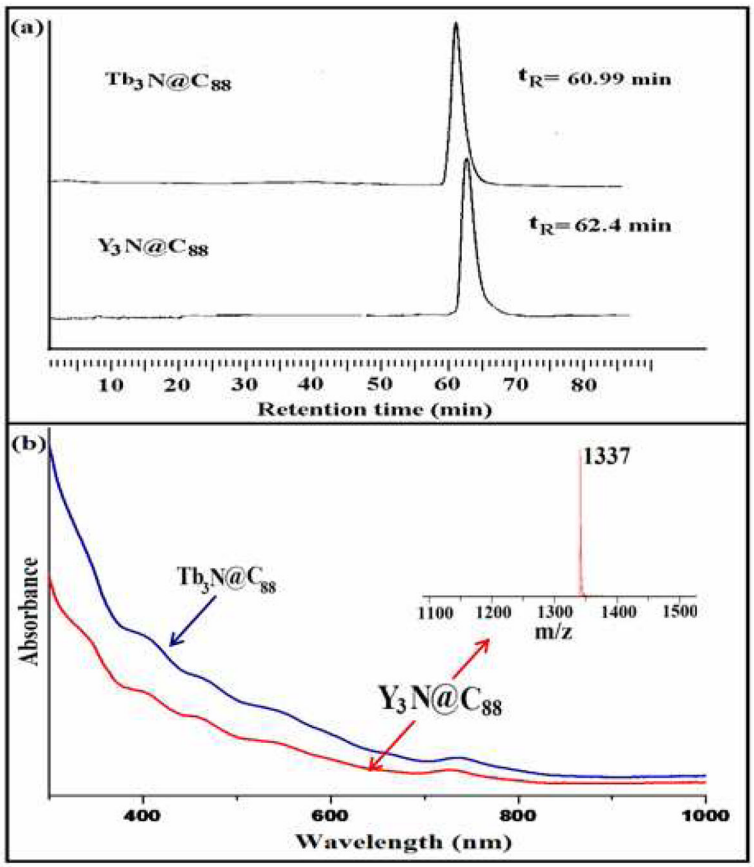

Figure 1.

(a) HPLC chromatogram of the purified $Y_3N@C_{88}$ and $Tb_3N@C_{88}$ (10 × 250 mm 5PYE column; λ=390 nm; flow rate 2.0 mL/min; toluene as eluent; 25 °C. (b) UV-vis spectra of $Y_3N@C_{88}$ and $Tb_3N@C_{88}$ in toluene and positive ion LD-TOF MS for purified $Y_3N@C_{88}$.

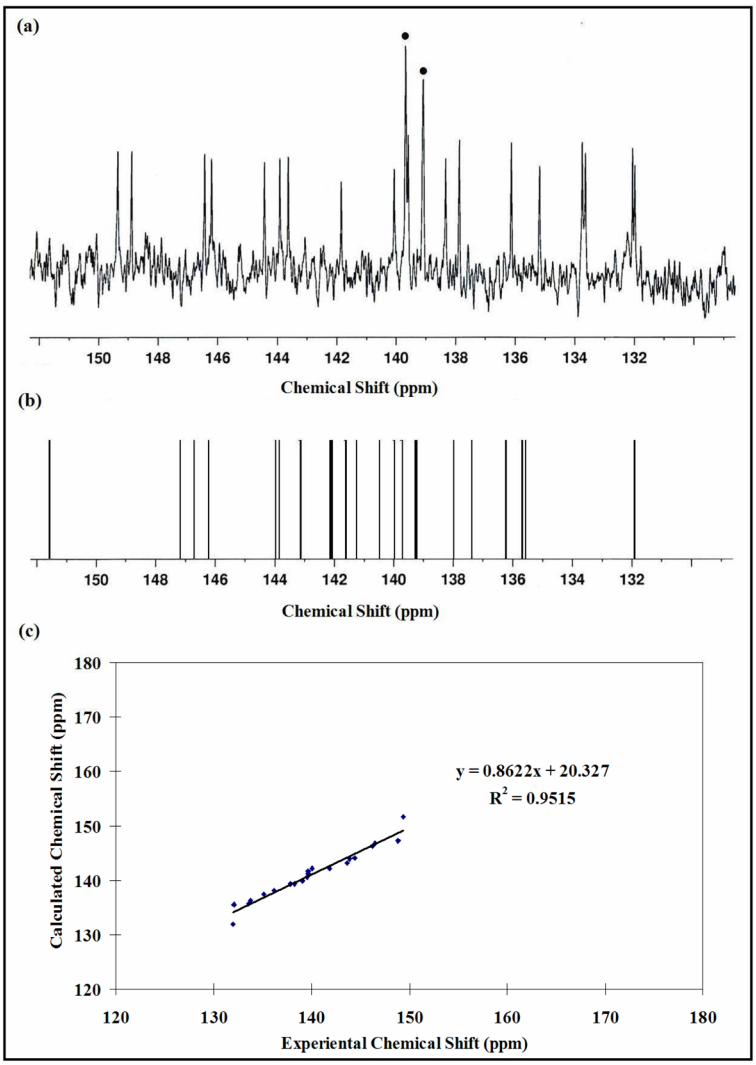

Figure 2.

(a)The ^{13}C NMR spectrum of $Y_3N@D_2$-C_{88} in CS_2 with 10 mg $Cr(acac)_3$ relaxant, acetone-d_6 lock) after 64,000 scan at 25 °C, showing the 22×4 pattern (number of NMR lines × relative intensity). The • corresponds to signal with double intensity. (b) Computational ^{13}C NMR spectrum for $Y_3N@D_2(35)$-C_{88}. The experimental and calculated ^{13}C shifts are provided in the SI. (c) Correlation between experimental and computational ^{13}C NMR results.

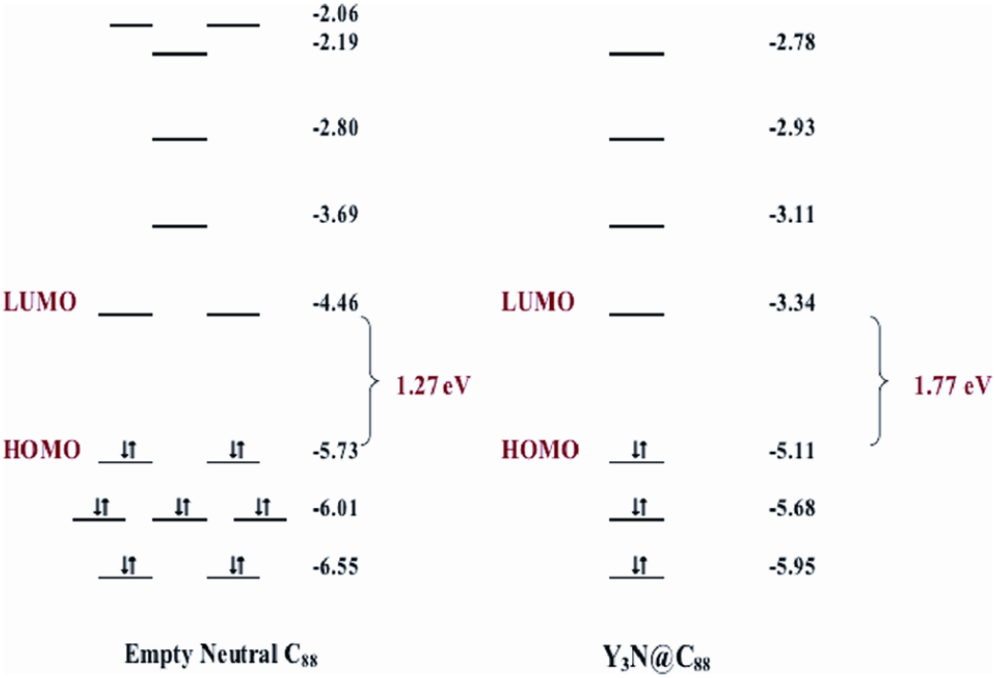

Figure 3.
DFT computational HOMO-LUMO levels for the neutral IPR D_2(35)-C_{88} and $Y_3N@D_2$(35)-C_{88} cages.

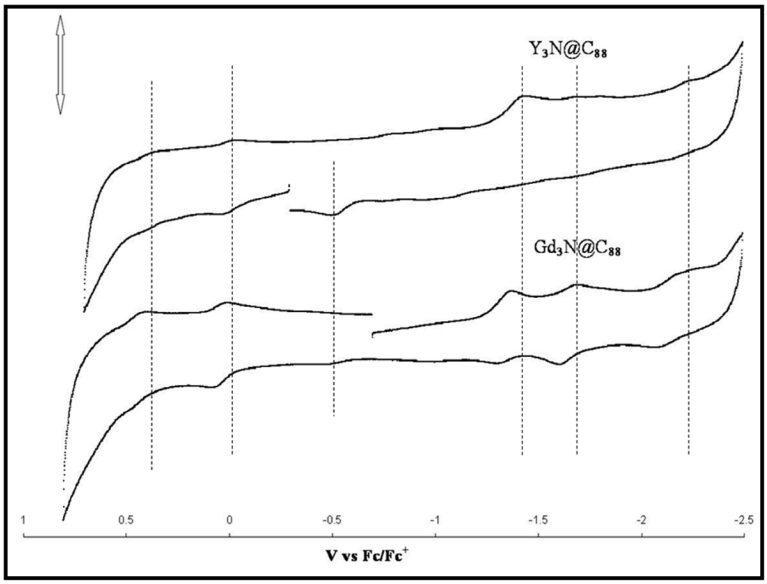

Figure 4.
Cyclic voltammogram of $Y_3N@C_{88}$ and $Gd_3N@C_{88}$; 100 mV/s; 0.1 M $TBABF_4$ in o-DCB.

Table 1

Redox potential of the $A_3@C_{2n}$ Endohedral Metallofullerenes

	$E_{1/2}^{ox1}$	$E_{1/2}^{ox2}$	E_{pc}^{red1}	E_{pc}^{red2}	ΔE_{gap}
$Y_3N@I_h$-C_{80}[15]	0.64		−1.41	−1.83	2.05
$Y_3N@C_{88}$	0.03	0.43	−1.43	−1.70	1.46
$Gd_3N@C_{88}$	0.05	0.45	−1.39	−1.71	1.44
$Gd_3N@C_{88}$[16]	0.06	0.49	−1.43	−1.74	1.49
$Nd_3N@C_{88}$[10]	0.07	0.53	−1.36	−1.75	1.43
$Pr_3N@C_{88}$[9]	0.09	0.54	−1.34	−1.72	1.43
$Ce_3N@C_{88}$[9]	0.08	0.63	−1.30	−1.57	1.38
$La_3N@C_{88}$[9]	0.21	0.66	−1.34	−1.67	1.57